

MRS Photodiode

D. Beznosko, G. Blazey, A. Dyshkant, K. Francis, D. Kubik, A. Pla-Dalmau, V. Rykalin, V. Zutshi

Abstract—In this article we show the latest results on the characteristics of the MRS (Metal/Resistor/Semiconductor) photodiode. They include measurements of noise vs. threshold characteristics, noise frequency and signal amplitude dependence on the applied voltage and temperature and irradiation dose, and stability as a function of time. The photoelectron separation for this sensor is measured using a signal from a Light Emitting Diode (LED). The response of the photodetector to light from the extruded 5mm thick long strips of scintillator is studied using cosmic ray muons. Also, fiber-sensor alignment effects were studied. The results are promising and illustrate the potential use of MRS as photosensors in wide range of detectors.

I. INTRODUCTION

All future detector (line Digital Hadron Calorimeter (DHC) [1] for a future e^+e^- linear collider) will require millions scintillating cells, possibly immersed in a strong magnetic field, and the same number of readout channels. This imposes strong constraints on the cost and performance of the photodetectors, which has directed our attention to the latest developments in this field. Newer detectors act as solid-state photo multipliers working in avalanche mode [2]. In spite of their relatively short history, these photodetectors may have an impact on the design of future detectors.

In this paper we have concentrated on the operating parameters and stability of the MRS; i.e., the dependence of amplification and noise count rate on the applied bias voltage, temperature and irradiation dose.

II. DETECTOR DESCRIPTION AND OPERATIONAL PRINCIPLES

The MRS photodiode is a multi-pixel solid-state device with every pixel operating in the limited Geiger multiplication mode. A resistive layer on the sensor surface achieves avalanche quenching. The device has a large number of pixels, ~ 1500 per 1×1 mm sensor [2]. The quantum efficiency (QE) of the device reaches 25% at 500nm [3].

III. EXPERIMENTAL SECTION

A. Working Point

For the MRS, amplification, QE, and intrinsic noise directly depend on the applied bias voltage, and this dependence differs for each individual photodetector. Thus, a particular bias voltage (working point) must be chosen for the above parameters.

For these tests, an 8-channel MRS board with preamplifiers from the Center for Perspective Technologies and Apparatus (CPTA) [2] was acquired (Fig. 1). First, all channels were tested under identical conditions; i.e., the same bias voltage and the same light signal from the green light emitting diode (LED) with peak emission at ~ 510 nm. The light from same LED was applied to each individual channel by physically switching position of the fiber, thus similar responses were expected. The disparity of response observed indicates that the optimal bias voltage must be found and tuned individually for each channel.

For further studies, channel #4 of the board was selected and a LeCroy [4] 623B octal discriminator and an ORTEC [5] 872 quad counter/timer were used to condition the signal. Most measurements were carried out at 22.6 ± 0.2 °C.

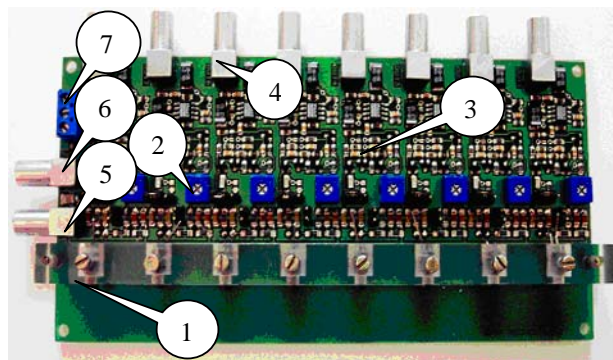


Fig. 1. Eight - channel MRS board: 1 – MRS sensor, 2 – bias voltage tuner, 3 – preamplifier, 4 – signal output, 5 – bias voltage input, 6 - test signal input and 7 - preamplifier power.

Manuscript received September 15, 2004. This work was supported in part by the U.S. Department of Education under Grant No. P116Z010035, the Department of Energy, and the State of Illinois Higher Education Cooperation Act.

A. Pla-Dalmau is with Fermi National Accelerator Laboratories, Batavia, IL 60510 USA (telephone: 630-840-3985, email: pla@fnal.gov).

D. Beznosko, G. Blazey, A. Dyshkant, K. Francis, D. Kubik, V. Rykalin, V. Zutshi are with Northern Illinois University, DeKalb, IL 60115 USA (telephone: 815-753-3504, email: rykalin@fnal.gov).

1) Working Point and Noise Count Rate

Three methods were used to determine a working point, or, rather, a working range for the device. For the first method, a low frequency (~150Hz) signal was applied to the LED that illuminates the photodetector through a clear fiber. This ensures that the bias voltage chosen will not only generate minimal noise but have 100% signal detection efficiency as well. The bias voltage was measured at the MRS directly. The preamplifier output was connected to a discriminator that, in turn, was connected to a counter/timer. Counts were accumulated over one minute period and converted into frequency. Fig. 2 shows the output signal frequency versus the bias voltage for a threshold value of 80mV. This values was chosen so that the amplitude of sensor's response is larger that the value of the threshold for the majority of the bias voltages. The plateau (from ~50.0V to ~51.0V) is a region of full signal detection with the least amount of internal noise, where amplification and QE increase towards the right side of the graph. Note that at higher bias voltages the curve starts to level again. This effect is due to the resistive layer at the top of the sensor that limits the gain and noise increase correspondingly. Gain limiting behavior will be illustrated in Subsection 2.

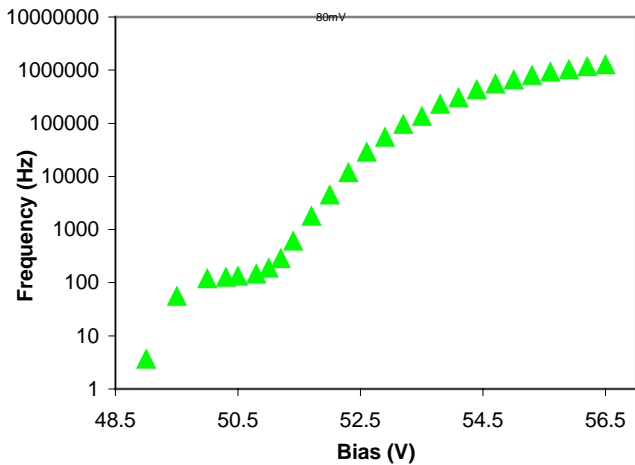


Fig. 2. Signal dependence on bias voltage at the thresholds of 80mV (~150Hz signal from LED is supplied to MRS).

2) Working Point and Amplification

For the second method of working point selection, a low amplitude signal of some frequency (the frequency is not important, thus the same ~150Hz signal was used here) was applied to the green LED (max in ~ 510nm), illuminating the photodetector through a clear fiber. Then the biasing voltage was changed, and the amplitude of the output signal was measured and plotted versus the bias voltage (Fig. 3).

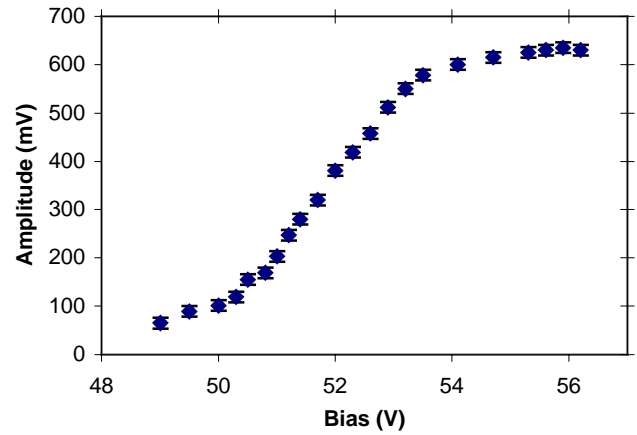


Fig. 3. Signal amplitude versus the bias voltage.

After some value of the bias voltage, a further increase in the voltage does not yield an increase in amplification. This indicated that gain is limited due to the resistive layer at the top of the sensor. This bias value can be also used as a definition of working point. However, at such high bias voltages the detector is close to the breakdown voltage; it generates high-frequency noise.

3) Working Point and Noise Amplitude

For the third method of selecting working point, the average amplitude of the dark noise of the sensor was measured separately with the LED turned off. Then the Signal-to-Noise (S/N) ratio was calculated at each corresponding value of the bias voltage, using the data acquired in this test and from Fig. 3. The results are plotted in Fig. 4; a distinct peak corresponds to the optimal balance between the level of sensor noise and amplification.

The bias voltage value for the MRS, obtained in this test, will be used for signal measurements for the further tests (unless noted otherwise). From Fig. 4 the optimal bias voltage for the MRS sensor used is 52.0V.

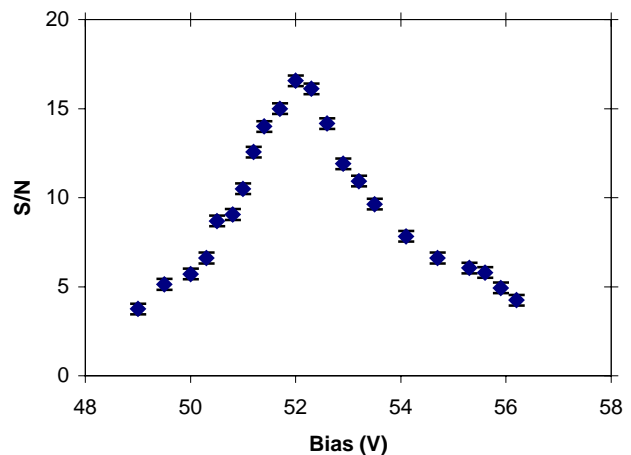


Fig. 4. Signal-to-noise value versus bias voltage for MRS.

B. Temperature and Irradiation Effects

The noise and signal dependence on temperature and the effects of radiation were measured. Here both the threshold of 80mV and the bias voltage of 51.3V were kept fixed throughout the test, with temperature the only variable. The exponential behavior of the noise frequency expected is illustrated in Fig. 5. The fit is added only to emphasize the exponential relationship between the noise frequency and the temperature.

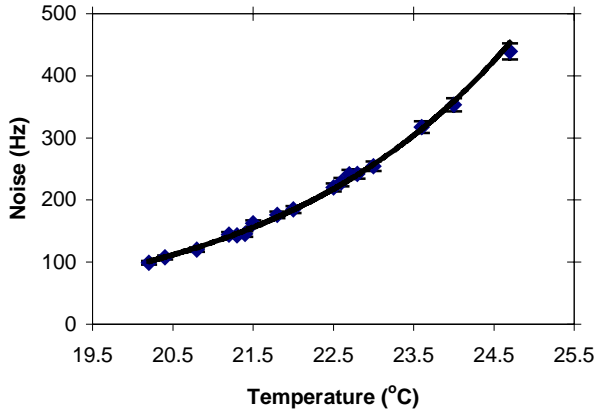


Fig. 5. Noise frequency versus temperature.

The amplitude dependence on temperature was also studied. The behavior of the signal amplitude seems to be linear for the range of the temperatures for which data was obtained, with ~3% change of the output amplitude per degree.

A separate study was undertaken to observe changes, if any, in the MRS sensor response after irradiation with a 1Mrad dose of gamma rays. The following parameters of the sensor: noise, amplification, signal detection, and bias voltage range for the sensor, were measured before and after the irradiation.

The comparison of “before” and “after” measurements indicated that a dose of 1Mrad gamma radiation causes no detectable damage to the sensor.

C. LED Measurements

The following were used to perform the calibration measurements with LED: a LeCroy [4] 623B octal discriminator, ORTEC [5] delay line, LeCroy [4] 2249A 12-channel ADC.

The MRS itself was biased at 52.0V. Fig. 6 shows the LED signal. We see a clear single-electron separation, and the first few Photoelectrons (PE) are easily distinguishable. The number of ADC channels between pedestal and first PE is the same as between first and second PE, and second and third PE.

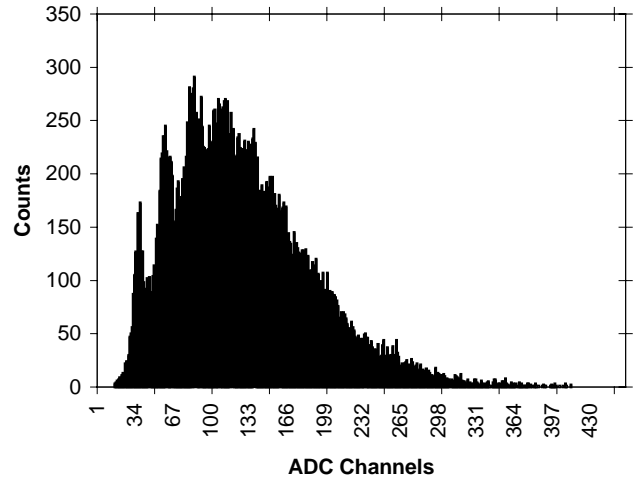


Fig. 6. MRS response to LED Signal. MRS was at 52.0V, gate of ~50ns used. Pedestal was in channel 38.

D. Cosmic Ray Measurements

The test was performed using scintillating strip with cosmic rays as the source of Minimum Ionizing Particles (MIPs). The strip used was made from extruded scintillator with co-extruded hole [7] along the strip, 1m long, 5cm wide and 5mm thick. 1.5m long KURARAY [6] Y-11, 1.0mm outer diameter, round, multicladd, WLS fiber with mirrored end, was embedded and glued, with 0.15m of fiber from the edge of the strip to the MRS. MRS was biased at 52.0V, gate of ~50ns and double-coincidence trigger of equal area were used. Fig. 7 shows the cosmic ray signal with the MRS. Using calibration data from the LED measurements for 1PE, we estimate the signal level at 17PE.

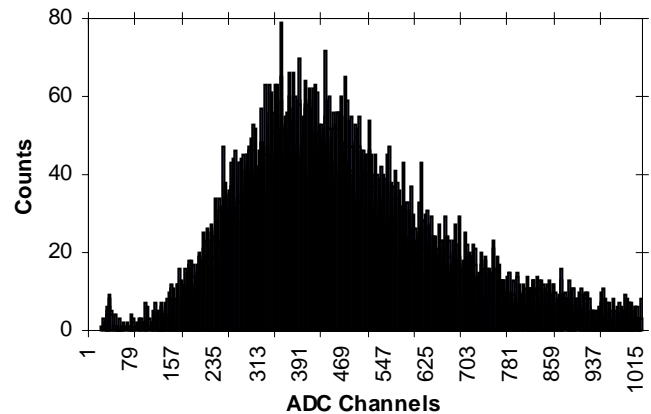


Fig. 7. MRS response to scintillating strip signal from cosmic rays. MRS was at 52.0V, gate of ~50ns used. Pedestal was in channel 38. Get 17PE.

E. Fiber Positioning and Sensor Response

The dependence of the output from MRS on the fiber alignment with the sensor was measured. Scans with fiber moving along, away and angled to the sensor were conducted.

Light signals from the green LED (peak emission at ~510nm) via 40 cm long 0.5mm outer diameter clear fiber were supplied to the MRS and readout was measured using a Tektronix [8] TDS2024 oscilloscope. Position and movements of the fiber with respect to the sensor were accomplished using Newport [9] 462 Series XYZ-M Integrated Linear Stage.

The scan was done along the sensor through its center (Fig. 8). A plateau corresponds to the region where the entire area of the fiber is within the photosensitive area of the sensor. Somewhat long tails on the far right and left sides are due to the light reflection off the protective shielding and the mount of the sensor, thus very small, but non-zero, value of the response is observed when the fiber moves completely away from the photosensitive area of the MRS. Another contributing effect is due to the fact that fiber is not pressed firmly onto the sensor area so that it could be moved along it without causing any damage. Hence, as the light signal exits the fiber, it forms a cone with larger cross-area at the surface of the sensor than the fiber itself would present. Precision of these measurements is approximately $\pm 12\text{mV}$ at each point. Positioning accuracy is ± 2.5 micron.

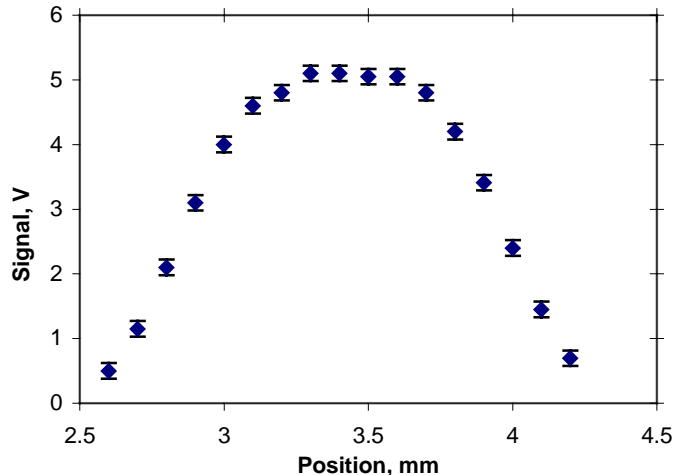


Fig. 8. Output signal amplitude versus position of the fiber along the MRS sensor.

IV. CONCLUSIONS

Measurements performed using cosmic rays with 1m long strip made of 5mm thick extruded scintillator allow clear distinction of the MIP signal.

Clear PE separation can be seen from the LED measurements. The device operates in the linear mode – each

photoelectron was separated from neighboring ones (or pedestal) by the same number of ADC channels.

At each given bias voltage the noise level can be greatly reduced by imposing a threshold. For instance, at the working point, the threshold at 1PE level reduces noise by a factor of 2500. Our study indicates that MRS noise is dominated by single PE noise. The radiation study shows that 1Mrad dose of gamma radiation has no noticeable effects on the MRS. Temperature measurements indicate a weak dependence of the output signal amplitude on temperature. The drop in noise frequency is exponential with temperature.

Tests of fiber misalignment with the sensor were carried out as well. The air gap of 0.5mm between the sensor and the fiber accounts for ~16% of signal loss.

As a result, we believe that MRS is a plausible photodetector for the scintillator-based multi-channel readout systems.

V. REFERENCES

- [1] A. Dyshkant, D. Beznosko, G. Blazey, D. Chakraborty, K. Frances, D. Kubik et al, "Small Scintillating Cells as the Active Elements in a Digital Hadron Calorimeter for the e+e- Linear Collider Detector", FERMILAB-PUB-04/015, Feb 9, 2004
- [2] V. Golovin et al., Limited Geiger-Mode Silicone Photodiode With Very High Gain. Nucl.Phys.Proc.Suppl. 61B: 347-352, 1998.
- [3] M. Golovin et al, "New Results on MRS APDS", Nucl. Instrum. Meth. A387:231-234,1997
- [4] LeCroy Corporation, 700 Chestnut Ridge Road, Chestnut Ridge, NY, 10977-6499
- [5] ORTEC, 801 South Illinois Avenue, Oak Ridge, TN 37830
- [6] Kuraray America Inc., 200 Park Ave, NY 10166,USA; 3-1-6, NIHONBASHI, CHUO-KU, TOKYO 103-8254, JAPAN.
- [7] Anna Pla-Dalmau, Alan D. Bross, Victor V. Rykalin, "Extruding Plastic Scintillator at Fermilab", FERMILAB-Conf-03-318-E, October 2003.
- [8] Tektronix Inc, 14200 SW Karl Braun Drive, P.O. Box 500, Beaverton, OR, 97077 USA.
- [9] Newport Corporation, 1791 Deere Avenue, Irvine, CA, 92606 USA.